London, Ser. A., **295**, 259, 271 (1966).
(6) D. Patterson, Y. B. Tewari, H. P. Schreiber, and J. E. Guillet, *Macromolecules*, **4**, 356 (1971).
(7) W. R. Summers, Y. B. Tewari, and H. P. Schreiber, *Macromolecules*, **5**, 12 (1972).
(8) (a) R. D. Newmann and J. M. Prausnitz, *J. Phys. Chem.*, **76**, 1492 (1972); (b) F. H. Covitz and J. W. King, *J. Polym. Sci., Polym. Chem. Ed.*, **10**, 689 (1972).
(9) A. B. Littlewood, "Gas Chromatography", Academic Press, New York, N.Y., 1970.
(10) J. E. Guillet, British Patent 1331429 (Sept. 26, 1973).
(11) J. E. Guillet, *J. Macromol. Sci., Chem*, **4**, 1669 (1970).
(12) J. E. Guillet, "Progress in Gas Chromatography", J. H. Purnell Ed., Wiley-Intersciences, New York, N.Y., 1973, p 187.
(13) R. L. Scott, *J. Chem. Phys.*, **17**, 279 (1949).
(14) P. J. Flory, "Principles of Polymer Chemistry", Cornell University Press, Ithaca, N.Y., 1953, p 495.
(15) (a) R. Foster, "Organic Charge-Transfer Complexes", Academic Press, New York, N.Y., 1969; (b) "Molecular Complexes", Crane, Russak and Co., New York, N.Y., 1973.
(16) P. J. Flory, *J. Am. Chem. Soc.*, **87**, 1833 (1965).
(17) P. J. Flory, R. A. Orwoll, and A. Vrig, *J. Am. Chem. Soc.*, **86**, 3515 (1964).
(18) B. E. Eichinger and P. J. Flory, *Trans. Faraday Soc.*, **64**, 2035, 2053, 2061, 2066 (1968).
(19) B. E. Eichinger and P. J. Flory, *Macromolecules*, **1**, 285 (1968).
(20) P. J. Flory, B. E. Eichinger, and R. A. Orwoll, *Macromolecules*, **1**, 207 (1968).
(21) P. J. Flory and H. Höcker, *Trans. Faraday Soc.*, **67**, 2258, 2270, 2275 (1971).
(22) L. P. McMaster, *Macromolecules*, **6**, 760 (1973).
(23) J. H. Purnell, "Gas Chromatography", Wiley, New York, N.Y., 1962.
(24) J. P. O'Connell and J. M. Prausnitz, *Ind. Eng. Chem., Process Des. Dev.*, **6**, 245 (1967).
(25) R. R. Dreisbach, "Physical Properties of Chemical Compounds", American Chemical Society Press, Washington, D.C., 1965.
(26) I. Timmermans, "Physico-Chemical Constants of Pure Organic Compounds", Elsevier, New York, N.Y., 1960.
(27) A. Bondi, *J. Phys. Chem.*, **68**, 441 (1964).
(28) R. D. Newmann and J. M. Prausnitz, *J. Paint Technol.*, **45**, 33 (1973).
(29) P. Doty, M. Brownstein, and W. Schlener, *J. Phys. Colloid Chem.*, **53**, 215 (1949).
(30) M. J. Schick, P. Duty, and B. H. Zimm, *J. Am. Chem. Soc.*, **72**, 530 (1950).
(31) C. E. H. Bawn and M. A. Wajid, *J. Polym. Sci.*, **12**, 109 (1954).
(32) J. H. Hildebrand, J. M. Prausnitz, and R. L. Scott, "Regular and Related Solutions", Van Nostrand, New York, N.Y., 1970.
(33) J. P. Sheridan, D. E. Martire, and Y. B. Tewari, *J. Am. Chem. Soc.*, **94**, 3294 (1972).
(34) J. P. Sheridan, D. E. Martire, and F. P. Banda, *J. Am. Chem. Soc.*, **95**, 4788 (1973).
(35) D. E. Martire and P. Riedle, *J. Phys. Chem.*, **72**, 3478 (1968).
(36) H. L. Liao, D. E. Martire, and J. P. Sheridan, *Anal. Chem.*, **45**, 2087 (1973).
(37) C. Booth and C. J. Devoy, *Polymer*, **12**, 309, 320 (1971).
(38) A. A. Jones, G. A. Brehm, and W. H. Stockmayer, "Princeton University Conference on Recent Advances in Polymer Science", Sept. 17 and 18, 1973.
(39) J. E. McGrath and M. Matzner, United States Patent 3,798,289 (March 19, 1974).
(40) J. V. Koleske and R. D. Lundberg, *J. Polym. Sci., Polym. Phys. Ed.*, **7**, 795 (1969).
(41) J. W. Gibbs, "The Scientific Papers of J. Willard Gibbs", Vol. I, Dover Publications, New York, N.Y., 1961.
(42) P. A. Small, *J. Appl. Chem.*, **3**, 71, 1953.
(43) M. T. Shaw, unpublished observations.
(44) T. K. Kwei, T. Nishi, and R. F. Roberts, *Macromolecules*, **7**, 667 (1974).
(45) R. N. Lichtenthaler, D. D. Liu, and J. M. Prausnitz, *Macromolecules*, **7**, 565 (1974).
(46) (a) R. Koningsveld, L. A. Kleintjens, and H. M. Schoffeleers, *Pure Appl. Chem.*, **39**, 1 (1974); (b) See "Note Added in Proof" of ref 46a.
(47) G. Allen, G. Gee, and J. P. Nicholson, *Polymer*, **2**, 8 (1961).
(48) D. McIntyre, N. Rounds, and E. Campos-Lopez, *Polym. Prepr., Am. Chem. Soc., Div. Polym. Chem.*, **10**, 531 (1969).
(49) D. G. Welygan and C. M. Burns, *J. Appl. Polym. Sci.*, **18**, 521 (1974).
(50) P. O. Powers, *Polym. Prep., Am. Chem. Soc., Div. Polym. Chem.*, **15**, 528 (1974).
(51) M. T. Shaw, *J. Appl. Polym. Sci.*, **18**, 449 (1974).
(52) B. Schneier, *J. Appl. Polym. Sci.*, **17**, 3175 (1973).
(53) O. Olabisi, in preparation.
(54) K. H. Reichert, *J. Oil Colour Chem. Assoc.*, **54**, 887 (1971).
(55) D. C. Bonner and J. M. Prausnitz, *Am. Inst. Chem. Eng. J.*, **19**, 943 (1973).
(56) G. Manzini and V. Crescenzi, *Polymer*, **14**, 343 (1973).
(57) J. J. Hickman and R. M. Ikeda, *J. Polym. Sci.*, **11**, 1713 (1973).
(58) D. D. Deshpande, D. Patterson, H. P. Schreiber, and R. S. Su, *Macromolecules*, **7**, 530 (1974).
(59) J. Scigliano, Sc.D. Thesis, Washington University, St. Louis, Missouri, 1972.
(60) C. E. H. Bawn, R. F. J. Freeman, and A. R. Kamaliddin, *Trans. Faraday Soc.*, **46**, 677 (1950).

The Cellulose Microfibril as an Imperfect Array of Elementary Fibrils

John Blackwell and Francis J. Kolpak*

Department of Macromolecular Science, Case Western Reserve University, Cleveland, Ohio 44106. *Received December 12, 1974*

ABSTRACT: Cellulose microfibrils are viewed as an imperfect array of elementary fibrils. We have investigated the possible defects in *Valonia* cellulose microfibrils, which are such that the microfibrils can be broken into elementary fibrils by deformation, but are not sufficient to allow for a small angle maximum corresponding to the elementary fibril dimension. The microfibril has been constructed by convolution of the elementary fibril with a two dimensional point lattice. Defects have been incorporated in the microfibril, first by introduction of gaps between the elementary fibrils. These regular gaps were then replaced by a statistical distribution of the elementary fibrils about the lattice points, modeled by Hosemann distortions of the first type. The cylindrically averaged transforms of such structures show that significant distortions can be incorporated within the microfibril without producing large scale changes in the equatorial intensity distribution. Larger distortions are necessary before a small angle maximum corresponding to the 35 Å elementary fibril is predicted, by which stage the wide angle X-ray pattern is unacceptable.

High resolution electron micrographs of negatively stained specimens of native cellulose[1-9] show that the microfibrils are comprised of regular subfibrils, termed "elementary" fibrils, which have a width of 35 Å. The major differences between celluloses from different sources occur in the packing of the elementary fibrils within the microfibril; this packing is expected to be dictated by the synthesis conditions. As an example, the microfibrils of *Valonia* (algal) cellulose have cross-sectional dimensions of ~200 × 100 Å. X-Ray line broadening measurements indicate that the microfibrils are essentially single crystals,[10,11] and thus the elementary fibrils must be arranged in a regular manner to give the larger crystallite width. If the elementary fibrils have cross sections 35 × 35 Å, the microfibril would correspond to a regular 6 × 3 array. In contrast, cotton microfibrils vary in width from ~100 to ~500 Å, with ~250 Å

being the average, whereas the calculated crystallite width from X-ray diffraction is ~60 Å. Crystallite widths which lie between the elementary and microfibril widths occur for most celluloses. It has been suggested that when the elementary fibrils are assembled to form the microfibril, some lateral fasciation occurs giving rise to the larger crystallites.[8] It is clear that many of the physical and mechanical properties of natural cellulose materials will depend on the nature of this array. In particular, we believe that many of the properties usually ascribed to low crystallinity and crystallite size can be explained by defects in the packing of elementary fibrils.

We have investigated the effects of such defects on the X-ray diffraction pattern of cellulose, starting with the *Valonia* microfibril structure. No one has ever observed small angle maxima corresponding to the 35 Å unit, for any native cellulose structure. This has led to attempts to dismiss the elementary fibril as a staining artifact for bundles of microfibrils, although such proposals are invalidated by observation of single 35 Å fibrils well separated from any aggregates. It is necessary therefore that the defects incorporated in the microfibril model be such that small angle maxima for the elementary fibril are not predicted. In micrographs of undeformed specimens, separate elementary fibrils are rare, and almost all the cellulose is in the form of aggregates. Nevertheless, these would not separate into regular subfibrils unless there were some differences between the center and faces of the elementary fibrils in the array. There could well be different packing or hydrogen bonding at the faces. Alternatively larger defects could be present such that failure occurs at these weak points and spreads like the opening of a zip-fastener when deformation occurs.

A fibrillar crystallite can be thought of as the convolution of a polymer chain, or the unit cell, with a two dimensional point lattice. The Fourier transform of the crystallite is given by

$$|F_{\text{crystallite}}| = |F_{\text{unit cell}}| \times |F_{\text{lattice}}| \quad (1)$$

i.e. the product of the Fourier transform of the unit cell and the lattice. $|F_{\text{unit cell}}|$ is given by

$$F(X, Y, l/c) = \sum_{j}^{n} f_j \exp[2\pi i(Xx_j + Yy_j + z_j l/c)] \quad (2)$$

where X and Y are the coordinates on the lth layer in reciprocal space and c is the fiber repeat; x_j, y_j, z_j are the atomic coordinates of the jth of n atoms in the unit cell. For a two dimensional point lattice consisting of N repeats of a and M repeats of b, $|F_{\text{lattice}}|$ is given by

$$|F_{\text{lattice}}(X, Y)| = \frac{\sin N\pi aX}{\sin \pi aX} \cdot \frac{\sin M\pi bY}{\sin \pi bY} \quad (3)$$

Equation 1 calculates the three dimensional transform for a fibrillar crystallite and needs to be squared and cylindrically averaged for comparison with a fiber diagram.

We will be concerned with the problems of packing fibrils together to form a larger crystallite. This can be achieved by convoluting the smaller fibril with a second lattice, and the Fourier transform for the larger fibril is given by

$$|F_{\text{large cryst}}| = |F_{\text{unit cell}}| \times |F_{\text{lattice 1}}| \times |F_{\text{lattice 2}}| \quad (4)$$

Where perfect lateral aggregation occurs, the repeats in lattice 2 are simple multiples of lattice 1, and the convolution is a one step rather than a two step process. However, we wish to consider the effect of distortions in the packing of elementary fibrils within a microfibril; i.e., lattice 1 is perfect but lattice 2 may contain relatively large distortions. As approximations for possible lattice distortions we have used two approaches. The first of these is a gap distortion or perfect lattice (PL) distortion. The conditions for perfect aggregation of small crystallites are $a_2 = N_1a_1$, $b_2 = M_1b_1$, where N_1 and M_1 are the number of repeats of a_1 and b_1, respectively, within the repeating distances a_2 and b_2 for lattice 2. In the PL distortion, $a_2 = N_1a_1 + \delta$ and $b_2 = M_1b_1 + \delta$, corresponding to gaps of δ between the elementary fibrils. This is not an unreasonable distortion and could occur in cellulose microfibrils, for example, if a layer of water molecules surrounded each elementary fibril. A more likely distortion, however, would be a statistical distribution of gaps between the elementary fibrils. This can be modeled as Hosemann distortions of the first type (H1)[12] by multiplication of the Fourier transform by an exponential term, $|F_{\text{distortion}}|$, corresponding to a crystallographic temperature factor. For the zero level plane in reciprocal space:

$$|F_{\text{distortion}}| = \exp-[(B/4)(X^2 + Y^2 + 2XY\cos\gamma^*)] \quad (5)$$

In eq 5, γ^* is the angle between the a^* and b^* axes and $B = 8\pi^2\bar{u}^2$, where $\bar{u}^2$ is the mean square displacement from the lattice point. $\bar{u}$ was taken as $\delta/3$; for a normal distribution the particles have a 99% chance of lying within $\pm\delta$ from the lattice point. Similar exponential terms should also be applied to allow for distortions within lattice 1 and within the unit cell. In applying a single $F_{\text{distortion}}$ term, the value of B contains the sum of the $\bar{u}^2$ values for distortions at the three levels. However, when the distortions in lattice 2 are much greater than those possible in lattice 1 and the unit cell, it is necessary only to consider the distortions in lattice 2 as a first approximation.

Application to Native Cellulose

Gardner and Blackwell[13,14] have refined the structure of native cellulose, based on the X-ray diffraction data for fibrous specimens from the cell walls of *Valonia ventricosa*. As originally proposed by Honjo and Watanabe[15] the unit cell is monoclinic with dimensions a = 16.34 Å, b = 15.72 Å, c = 10.38 Å (fiber axis), and γ = 97.0°; the cell contains sections of eight chains. Nevertheless, a two chain monoclinic unit cell with dimensions a = 8.17 Å, b = 7.86 Å, c = 10.38 Å, and γ = 97.0°, and space group $P2_1$, like the unit cell due to Meyer and Misch,[16] was adequate for structure refinement. Rigid-body least-squares refinement showed that the structure consists of chains with the same sense (parallel). The ab projection of the structure is shown in Figure 1. The chain through $a/2$, $b/2$, 0 is shifted by 0.266c with respect to the chain through the origin; the rotations of the two chains about the fiber axis are identical. Sarko and Muggli[17] have also proposed parallel chain structures for cellulose. In addition to the structure described above they have considered a triclinic unit cell with successive chains along the diagonal in the eight chain cell being displaced by c.4, $c/2$, and $3c/4$. However, the two structures are identical in the ab projection, and the treatment of the $hk0$ data below is not dependent on this choice of model.

Preston and Cronshaw[19] and Preston et al.[18] found that the 6.1 Å planes ($1\bar{1}0$) of cellulose are parallel to the flattened faces of the microfibrils. Hence, Frey-Wyssling's model of the elementary fibril and microfibril has the sides corresponding to the 110 and $1\bar{1}0$ planes of the Meyer and Misch unit cell.[20,21] For this reason it was convenient to define a new unit cell with a and b axes corresponding to the diagonals of the Meyer and Misch (MM) unit cell, similar to that proposed by Ellis and Warwicker.[22] This larger (EW) unit cell is also shown in Figure 1; the dimensions are

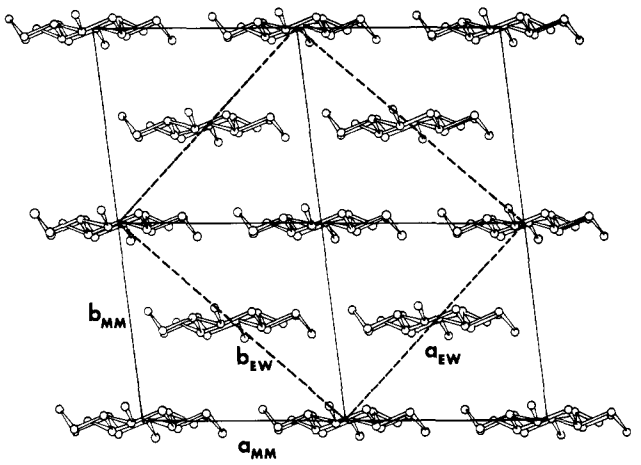

Figure 1. *ab* projection of the crystal structure of native cellulose.[14] The projection shows four MM unit cells, e.g., one EW unit cell; the EW unit cell used for the calculations is also shown and has *a* and *b* axes (dotted lines) corresponding to the diagonals of the MM unit cell.

a = 10.62 Å and b = 12.00 Å.

The elementary fibril can now be constructed by convolution of the contents of the EW unit cell with a 3 × 3 lattice with the same a and b dimensions giving cross-sectional dimensions a_{EF} = 31.86 Å and b_{EF} = 36.00 Å. The microfibril was then constructed by convolution of this elementary fibril with a 6 × 3 lattice with dimensions a_{EF} and b_{EF}. The cross-sectional dimensions of the microfibril are a_{MF} = 191.16 Å and b_{MF} = 108.00 Å. Alternatively, the microfibril can be built up by convolution of the EW unit cell with an 18 × 9 lattice to give the same structure. The model for the perfect microfibril as a 6 × 3 array of elementary fibrils is shown in Figure 2, where the structure of the elementary fibril, as a 3 × 3 array of EW unit cells, each containing four chains, is also depicted.

The above model for the elementary fibril contains 6 × 6 = 36 chains, whereas that proposed by Frey-Wyssling and Muhlethaler[8] contained an extra layer of chains along one axis, i.e., 7 × 6 = 42 chains. Both elementary fibrils are within experimental error of the observed dimension of 35 Å, but our microfibril is a shade small at 191 Å compared to the observed width of 200–210 Å. However, the choice of model is not critical to any of the conclusions below for distorted lattices, and selection of the 6 × 6 elementary fibril simplifies the calculations by avoiding a change of axis. Furthermore, insertion of distortions will increase the size of the microfibril.

Our model also differs from that proposed by Haase[23] et al. from investigation of paracrystalline distortions of ramie and viscose fibers. In their interpretation of the small angle X-ray data for ramie cellulose, they assumed a cylindrical cross section for their fibrillar units, and proposed a structure consisting of 52 Å diameter rods and aggregates thereof. This model is not consistant with electron microscope observations for ramie fibers: 52 Å rods have not been observed although reports of smaller 35 Å units have been published.[24] Apart from the larger basic unit, however, the Haase model is similar to ours, with larger aggregates built up from a basic subunit.

Zero level transforms were calculated for the four chain EW unit cell using the atomic coordinates of the carbon and oxygen atoms.[14] The transform of the elementary fibril was calculated using eq 1–3; in eq 3, N = 3, M = 3, a = 10.62 Å, and b = 12.00 Å. Similarly, the transform of the perfect microfibril was calculated using eq 3 and 4, inserting values N = 6, M = 3, a = 31.86 Å, and b = 36.00 Å. In

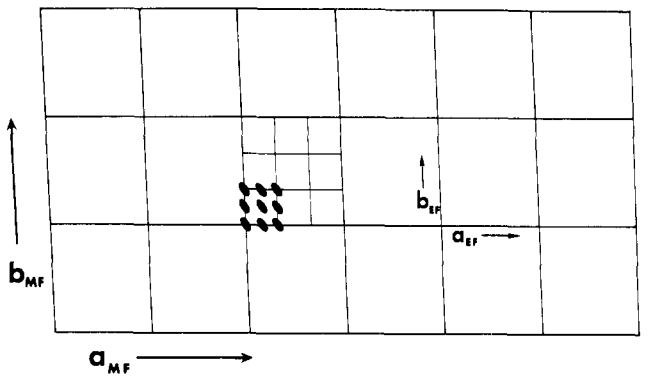

Figure 2. Idealized assembly of a *Valonia* cellulose microfibril as a perfect 6 × 3 array of elementary fibrils, which in turn are perfect 3 × 3 arrays of EW unit cells. The chains in an EW unit cell are represented by ellipses.

all cases the transforms were calculated for points on an a^*b^* grid separated by 0.01 Å^{-1}, except below R = 0.1 Å^{-1} ($R = (X^2 + Y^2)^{1/2}$), where the grid increments were 0.001 Å^{-1}, allowing for adequate resolution in the small angle region. Cylindrically averaged transforms were computed by averaging the values of F within increments of R = 0.01 Å^{-1} (0.001 Å^{-1} below R = 0.1 Å^{-1}).

Results

Figure 3 shows the cylindrically averaged transforms of the four chain unit cell (a), elementary fibril (curve b) and perfect *Valonia* microfibril (curve c). The transform for the elementary fibril shows a small angle minimum at R = 0.0320 Å^{-1} (d = 31.2 Å) followed by a sharp peak at R = 0.0414 Å^{-1} (d = 24.1 Å). If the elementary fibril is approximated by a solid cylinder of equal volume, such a cylinder would have radius r_0 = 19.10 Å. The Fourier transform for a solid cylinder is

$$F(R) = r_0 J_1(2\pi R r_0)/R \qquad (6)$$

The first zero and maximum for $F(R)$, corresponding to the first intensity minimum and maximum, occur at R = 0.0327 Å^{-1} and R = 0.0433 Å^{-1} for r_0 = 19.10, which are very similar to the figures calculated for the fibril model. As expected, the small angle region can be predicted from the transform of a rectangular rod. A maximum should be seen at approximately 24 Å for a specimen made up of unaggregated elementary fibrils. Microscopy, however, shows that individual elementary fibrils comprise an extremely small fraction of the observed morphology in undeformed specimens, which are almost entirely aggregates, with a result that the 24 Å maximum is not observed.

Transition to the perfect microfibril (curve c, Figure 3) sharpens the peaks considerably. This transform is very similar to the observed equatorial intensity distribution, which is shown in Figure 3 (curve d). The first three peaks at d = 5.96, 5.23, and 3.85 Å correspond to the $1\bar{1}0$, 110, and 020 reflections (MM unit cell indexing). The peak heights match the structure factors calculated for these reflections for the infinite lattice by Gardner and Blackwell.[14] The 24 Å peak is naturally not seen for the microfibril due to perfect aggregation. The question as to what degree of imperfection is necessary to generate this peak will be considered below.

The major features of the cellulose equatorial pattern (Figure 3, curve d) are seen in the transform of the four chain unit cell. On going to the elementary fibril, a change occurs in the relative intensity of the first two (wide angle) peaks, and the 24 Å equatorial is produced. For the microfibril the peaks are sharpened considerably and the first

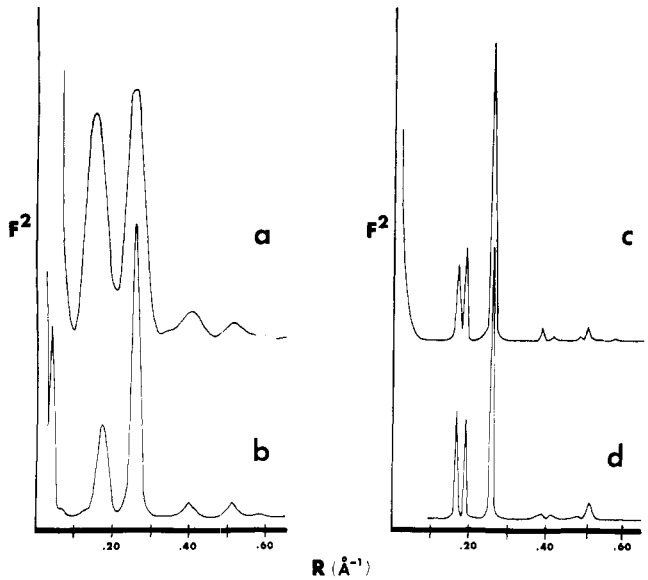

Figure 3. Cylindrically averaged zero level squared Fourier transforms for (a) four chain unit cell, (b) the elementary fibril, and (c) the perfect microfibril. For comparison (d), the corrected intensity distribution from a densitometer scan through the equator of a *V. ventricosa* fiber pattern.

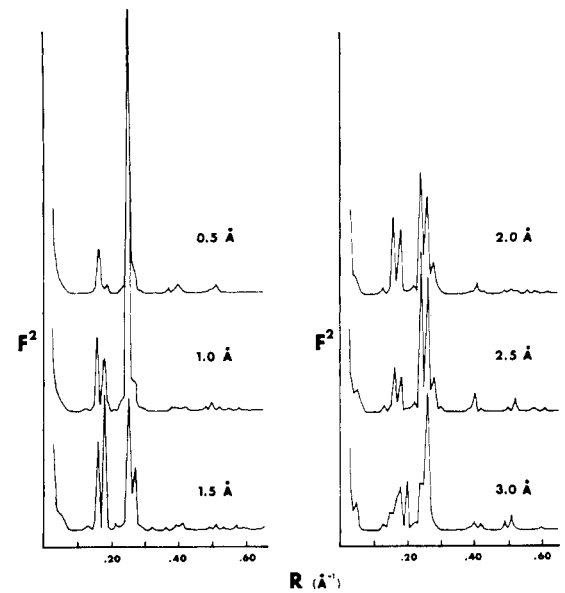

Figure 4. Zero level cylindrically averaged squared Fourier transforms of the microfibril with various PL distortions.

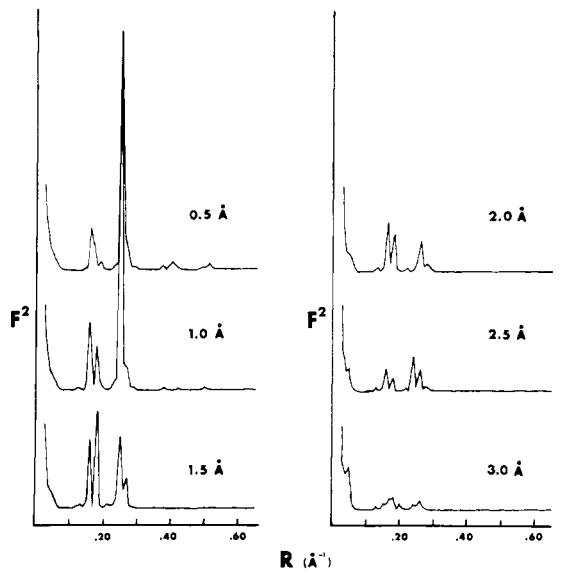

Figure 5. Zero level cylindrically averaged squared Fourier transforms of the microfibril with various H1 distortions.

peak of the elementary fibril is split into two. The three intense peaks of the microfibril are the $1\bar{1}0$, 110, and 020 peaks (MM unit cell).

Distortions

The zero level cylindrically averaged transforms for microfibrils containing perfect lattice distortions are shown in Figure 4 where the curves correspond to δ values of 0.5, 1.0, 1.5, 2.0, 2.5, and 3.0 Å, respectively. The effect of this straightforward expansion of the microfibril lattice is to vary the relative intensities of the peaks. The position of the peaks also varies slightly, since the repeats for lattice 2 have been changed by δ.

For the 0.5 Å PL distortion the intensity of the 110 peak is reduced, and compares unfavorably with the transform of the undistorted lattice. However, for the 1.0 Å PL distortion intensity is restored to the 110 peak. The intensity ratio of the $1\bar{1}0$ and 110 peaks is reversed, compared to the transform of the perfect microfibril. However, this is closer to the distribution on the X-ray pattern. Aside from the increased intensity for the 020 peak, the transform gives a reasonable intensity distribution. The transforms for the 1.5, 2.0, 2.5, and 3.0 Å PL distortions are drastically different from the first two and show almost no resemblence to the observed intensity distribution.

A weak maximum is seen in the small angle region for the 2.5 and 3.0 Å PL distortions corresponding to the repeat for the elementary fibril. This peak becomes only a shoulder for the 1.5 and 2.0 Å PL distortions and nothing is seen for gaps of 1.0 and 0.5 Å. It is clear then that relatively large gaps between the elementary fibrils would be necessary to give small angle activity, by which time the wide angle pattern is unreasonable. In actual specimens the gaps between elementary fibrils will not be empty spaces but will be filled, e.g., with water, which will reduce the intensity calculated for the small angle peak.

A better model for the imperfect packing of elementary fibrils incorporates the Hosemann type one (H1) distortions, which allow for statistical deviations from the perfect lattice points. This is achieved by multiplying the PL transform by the exponential term in eq 5. The transforms obtained are shown in Figure 5. The distortion term is analogous to a temperature factor and simply reduces the relative intensities as R increases. This has the effect of decreasing the intensity of the 020 reflection relative to the $1\bar{1}0$ and 110 reflections, with a result that the 1.0 Å H1 distortion becomes a reasonable match to the observed data. The values of $\bar{u}^2$ used in the present calculations for $\delta > 1.0$ Å are significantly larger than that indicated by the refin d temperature factor for *Valonia* cellulose,[14] but are probably not unreasonable for less ordered cellulose structures.

Conclusions

Fourier transforms have been calculated for cellulose microfibrils built up as perfect or disordered arrays of elementary fibrils. The transforms for *Valonia* microfibrils showed that significant distortions could be introduced in the array of elementary fibrils, without drastically affecting the wide angle X-ray pattern. Larger distortions were necessary before a small angle maximum was predicted, by which time the wide angle pattern was unreasonable. In-

deed, the 1.0 Å gaps within the *Valonia* coupled with the H1 distortion gave better agreement than the perfect crystallite for the relative intensities of the $1\bar{1}0$ and 110 reflections. This reversal of intensities is of interest since such differences in these relative intensities and slight differences in the positions of the three strong reflections have been observed for unoriented specimens of native cellulose from different sources. It is also interesting to note that insertion of one water molecule per chain between faces of the elementary fibril would produce an expansion of approximately 1 Å. As an analogy, conversion of anhydrous β-chitin to the monohydrate increases the lateral lattice parameter from 9.3 to 10.3 Å.[25] An imperfect layer of water molecules between the elementary fibrils would thus be an acceptable distortion.

The defects within the microfibril could be modeled more closely by Hosemann type two (H2) distortions,[12] incorporating possible turns about the fiber axis. The H2 distortions would have the effect of broadening the reflections with increasing scattering angle, but for a system as nearly perfect as *Valonia* cellulose, the use of H1 model is probably adequate. For less ordered systems such as cotton cellulose the reflections are much broader and it is likely that H2 distortions will need to be incorporated. Such studies are currently in progress for cotton, where the higher layer line data are also being used to investigate elementary fibril displacements parallel to the fiber axis.

Acknowledgment. This research was supported by NSF Grant No. GH34227 and N.I.H. Research Career Development Award No. AM80642 (to J. Blackwell).

References and Notes

(1) K. H. Gardner and J. Blackwell, *J. Ultrastruct. Res.*, **36**, 725–731 (1971); *J. Polym. Sci., Polym. Symp.*, **No. 36c**, 327–340 (1971).
(2) F. J. Kolpak and J. Blackwell, *Text. Res. J.*, in press.
(3) K. Muhlethaler, *Beih. Z. Schweiz. Forstver.*, **30**, 55 (1960).
(4) A. N. J. Heyn, *J. Ultrastruct. Res.*, **26**, 52–68 (1969).
(5) A. Frey-Wyssling, K. Muhlethaler, and R. Muggli, *Holz Roh Werkst.*, **24**, 443–444 (1966).
(6) I. Ohad and D. Dannon, *J. Cell Biol.*, **22**, 302–305 (1964).
(7) A. N. J. Heyn, *J. Appl. Phys.*, **36**, 2088 (1965).
(8) A. Frey-Wyssling and K. Muhlethaler, *Makromol. Chem.*, **62**, 25–30 (1963).
(9) G. Cox and B. Juniper, *J. Microsc. (Oxford)*, **97**, 343–355 (1973).
(10) I. Nieduszynski and R. D. Preston, *Nature (London)*, **225**, 273–274 (1970).
(11) D. Caulfield, *Text. Res. J.*, **41**, 267–269 (1971).
(12) R. Hosemann and S. N. Bagchi, "Direct Analysis of Diffraction by Matter", North-Holland Publishing Co., Amsterdam, 1962.
(13) K. H. Gardner and J. Blackwell, *Biochem. Biophys. Acta*, **343**, 232–237 (1974).
(14) K. H. Gardner and J. Blackwell, *Biopolymers*, **13**, 1975–2001 (1974).
(15) G. Honjo and M. Watanabe, *Nature (London)*, **181**, 326–328 (1958).
(16) K. H. Meyer and L. Misch, *Helv. Chem. Acta*, **20**, 232–244 (1937).
(17) A. Sarko and R. Muggli, *Macromolecules*, **7**, 486–694 (1974).
(18) R. D. Preston, et al., *Nature (London)*, **162**, 665–667 (1948).
(19) P. D. Preston and J. Cronshaw, *Nature (London)*, **181**, 248–250 (1954).
(20) A. Frey-Wyssling, *Science*, **119**, 80–82 (1954).
(21) A. Frey-Wyssling, *Biochem. Biophys. Acta*, **18**, 166–168 (1955).
(22) E. C. Ellis and J. O. Warwicker, *J. Polym. Sci.*, **56**, 339–357 (1962).
(23) J. Haase, R. Hosemann, and B. Renwanz, *Kolloid Z. Z. Polym.*, **251**, 871–875 (1973).
(24) A. N. J. Heyn, *J. Cell Biol.*, **29**, 181–197 (1966).
(25) J. Blackwell, *Biopolymers*, **7**, 281–298 (1969).

The Effect of Surface Adsorption on Gas Chromatographic Measurements Near Polymer Melting Transitions

G. Courval and D. G. Gray*

Pulp and Paper Research Institute of Canada, and the Department of Chemistry, McGill University, Montreal H3C 3G1, Canada. *Received January 25, 1975*

ABSTRACT: The extension of gas chromatographic methods to studies on the interaction of polar polymers and vapors is complicated by adsorption at the polymer–vapor interface. Some effects of this adsorption were examined using water and *n*-propyl alcohol as probes with a poly(ethylene oxide) stationary phase coated onto an inert fluorocarbon support. The measured retention volumes depended markedly on the surface-to-volume ratio of the stationary phase, in a manner consistent with independent surface and bulk contributions to the retention mechanism. Using an extrapolation procedure, the true bulk retention volumes for poly(ethylene oxide) above and below its melting point were determined. The crystallinity of the polymer, estimated from these data, was found to be in good agreement with previously reported values. It is concluded that in order to interpret correctly GLC retention data near a polymer melting region, both exclusion of the vapor from crystalline regions and surface adsorption must be considered.

The application of gas chromatography to physicochemical measurements [1,2] has proven useful in several areas of polymer science.[3] Perhaps the most fruitful area has been the derivation of thermodynamic information on polymer–solvent interactions at low solvent concentrations.[3,4] For relatively nonpolar vapors and polymers, at temperatures substantially above the melting point or glass transition temperature, equilibrium thermodynamic parameters may be derived with some confidence from appropriately corrected[1] gas chromatographic data.

Gas chromatography has also been used to study polymer phase transitions. The GC retention volume[1–3] reflects the interaction of a "probe" vapor with the polymer; changes in the polymer structure which occur at the melting point or the glass transition temperature should therefore exert a marked effect on the retention volumes. Sharp discontinuities have been detected in the variation of retention volumes with temperature for hydrocarbons on columns containing polyethylene and polypropylene near the polymer melting points.[5] This work was extended by Guillet and coworkers who determined melting points, degrees of crystallinity, and crystallization kinetics for polyolefins by GC.[6] Glass transition temperatures of poly(*N*-isopropyl acrylamide),[7] poly(styrene), poly(vinyl chloride), poly(methyl methacrylate),[8] polycarbonates[9] and poly(acrylonitrile)[10] were also detected by this method. Gas chromatographic evidence has been presented for a second-order transition other than the glass transition in cellulose acetate.[11] Phase transitions of organic compounds and liquid crystals have also been widely dealt with in the gas chromatographic literature, mainly with a view to their possible usefulness in improving separations.[12] In particular, the